IGC-113
1990

IGC-113
1990

Glow Discharge Lamp A Light Source For Optical Emission Spectroscopy

K.S. Viswanathan
V. Srinivasan
S. Nalini
T.R. Mahalingam

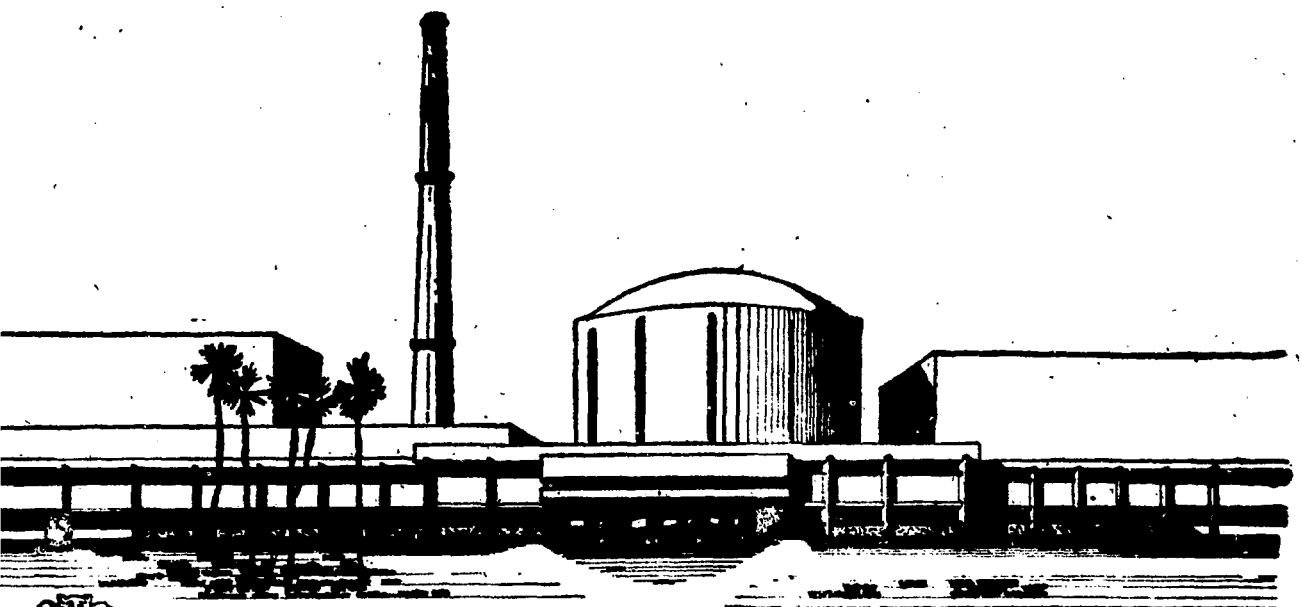

GOVERNMENT OF INDIA. DEPARTMENT OF ATOMIC ENERGY
INDIRA GANDHI CENTRE FOR ATOMIC RESEARCH KALPAKKAM

IGC--113
1990

GOVERNMENT OF INDIA

DEPARTMENT OF ATOMIC ENERGY

GLOW DISCHARGE LAMP
A LIGHT SOURCE FOR OPTICAL EMISSION SPECTROSCOPY

K.S. Viswanathan, V. Srinivasan, S.Nalini and T.R.Mahalingam

Indira Gandhi Centre for Atomic Research

Kalpakkam 603 102, Tamil Nadu, India

CONTENTS

ABSTRACT

A glow discharge lamp based on a modified version of the Grimm design has been fabricated in our laboratory. We have demonstrated its utility as a radiation source for optical emmission spectrography by standardising a method for the analysis of low alloy steels using a set of certified standards from DMRL, Hyderabad.

We have also proposed a model where we have correlated the sputtering rates of different metals with their heats of sublimation, metallic radii and densities. Sputtering rates of ten different metals obtained from literature have been used to test this model, and the correlation appears to be excellent.

GLOW DISCHARGE LAMP
A LIGHT SOURCE FOR OPTICAL EMISSION SPECTROSCOPY

K. S. Viswanathan*, V. Srinivasan*, S. Nalini*, and T.R.Mahalingam*

I. INTRODUCTION:

Over the last two decades the glow discharge (GD) source has become increasingly popular as an emission source for analytical spectroscopy[1-6]. The GD source is not just another addition to the list of radiation sources that an analytical spectroscopist can reach out for, but has certain unique features which make it convenient in the analysis of solid samples. It has also gained immense utility in corrosion studies of solids, since it offers the possibility of obtaining concentration profiles of various elements as a function of depth in the solid[7-9].

The first observations of optical phenomena in low pressure gas discharges date back to the nineteenth century, following the work of Hittorf and Crookes[10]. However, the impetus for the development of the GD source as an analytical tool was received only after Grimm[11] developed his flat-cathode source in 1968. The novelty of the Grimm source was in the fact that the discharge was simultaneously obstructed and abnormal, and resulted in a high sputtering yield of the sample. Other designs followed, where an auxiliary high frequency discharge (RF

---

*Radiochemistry Programme, Indira Gandhi Centre for Atomic Research, Kalpakkam 603 102

or Microwave) was used to augment the emission from a Grimm type GD source[4,12]. An excellent review of the developments in GD sources has been presented by Caroli[13].

Low pressure gas discharges are produced using a cell filled with an inert gas, say argon, at a pressure of 1-10 torr. The gas cell is provided with two electrodes, across which a DC voltage V is applied through a current limiting resistor R. As long as the applied voltage V, is less than V_b, the breakdown voltage, no continuous current will be observed, unless an external source of current, like X-ray induced photoelectrons from the cathode, is used. As the voltage is raised slowly, a dark self-sustaining discharge is produced when the voltage attains the value V_b. Such a discharge is called the Townsend discharge, characterised by currents of the order of 10^{-6} A. If the current is now increased, the voltage stays steady for some time, shown as region AB in Fig. 1, and then starts falling through the region BC and reaches a constant value of V_n at the point C. At this point a visible glow appears. Further increase in current produces no increase in voltage (region CD). This region is known as the normal glow region. This is followed by the abnormal glow (region DE) where the voltage increases with increase in current. The transition from the normal glow to the abnormal glow results from the cathode area being current saturated. The abnormal glow is characterised by high sputtering efficiencies of the cathode material. Further increase in current results in an arc discharge (region EF).

A typical low pressure gas discharge is marked by a number of dark and luminous zones [14]. Close to the cathode is

a dark layer called the Aston dark space, characterised by the presence of low energy electrons. This is followed by a weakly luminiscent cathode layer, and then a second dark layer called the Crooke or Hittorf dark space. Following this is a strong luminous zone called the negative glow. The luminosity of this zone results from the numerous electrons produced from the ionization processes occuring in the cathode dark space, as well as by the few faster ones originating from the cathode. Positive ions are also generated, which accelerated by the cathode fall, crash into the cathode and sputter the cathodic material. This sputtered material then enters the negative glow. The negative glow, therefore, consists of a mixture of atoms of Ar and the cathodic material and is the zone of interest where an analysis of the cathode sample is required. Following the negative glow, we have the Faraday dark space and the positive column. The positive column is not essential in sustaining the discharge nor does it contain any useful information of the cathodic material. It is for this reason that the Grimm source uses an obstructed glow configuration, where the anode is brought so close to the cathode, that the positive colum is completely eliminated and the discharge is dominated by the negative glow.

Sputtering is therefore the basic mechanism in the glow discharge, which transports the atoms of the cathode material to the discharge zone, especially when the lamp is operated in the abnormal glow region. Since the process of sputtering removes the material from the cathode, layer by layer, the low presurre abnormal glow discharge source can be used to obtain

concentration profiles of materials as a function of depth in the solid. The sampling of the cathodic material by sputtering is also generally free from matrix effects. These are the unique features that have made the glow discharge lamp a useful and a unique analytical tool.

Our interest in the glow discharge lamp is twofold: 1) for use as an analytical tool for the analysis of solid samples, and 2) for use in corrosion studies where concentration profiles of various elements as a function of depth is required.

II. DESIGN OF THE GLOW DISCHARGE LAMP:

Our initial version of the glow discharge lamp was based on the design on Mavrodineanu[14]. This design uses an alumina disc as an insulator between the cathode and anode and also serves to hold the sample in position. As an alumina disc of the specific shape and size was not readily available, we substituted it with perspex. However, the proximity of the perspex disc to the discharge zone and the improper cooling of the sample charred portions of the perspex. We therefore had to modify the design of the lamp.

We redesigned the cathode assembly and the present version of our lamp is shown in Fig. 2. The sample, which acts as the cathode itself, and hence has to be electrically conducting, is mounted on the sample holder and secured in place by a pyrofillite cap. The sample holder moves through a stainless steel flange on a fine pitch screw (0.6 mm pitch), which allows for exact adjustment of the anode-cathode spacing. The stainless

steel flange is mounted on a perspex body, whose internal diameter is kept large enough, so its proximity to the discharge zone is avoided. The anode consists of a cone shaped ring, mounted on a hollow cylindrical body, both made of Cu-Be alloy. The anode body has a gas inlet port, a quartz window to couple light onto a spectrograph and a terminal for power supply. Since in our configuration, the anode is maintained at voltages ranging from 500 V to 1 kV, the anode body is enclosed in a nylon jacket for operator safety. The cathode is grounded, and hence has no protective shroud. Cooling of the lamp is effected by water circulating through the anode body and the sample holder. The entire system is evacuated with a rotary pump. The operating pressure of the lamp (typically 1-10 torr) is measured using an oil manometer.

III. EXPERIMENTAL:

The lamp is operated by first evacuating to a base pressure of 150 microns of Hg. The system is then flushed by letting in high purity Argon (IOLAR 1) to a few torr and evacuating again down to 150 microns. This is repeated a few times. Argon (IOLAR 1) is then leaked into the system and the flow rate is adjusted with the help of needle valves to obtain the desired operating pressure in the lamp. The lamp is then connected through a current limiting resistor of 1 K ohm (100 W) in series to a DC power supply capable of providing a maximum current of 200 mA and a potential of 1 kV. Light from the discharge is focussed with the help of a 100 mm focal length

quartz cylindrical lens onto the slit of a 3.4 m Ebert mount Jarrel-Ash spectrograph (Fig. 3). A 590 grooves/mm or a 1180 groves/mm grating is used, depending on the resolution required in the particular experiment. With a 590 grooves/mm grating the reciprocal dispersion turns out to be 5 Å/mm. Most of the experiments described in this report were perfomed with the 590 grooves/mm grating. The spectra were recorded on Kodak SA1 photographic plates with typical exposure times ranging from 2 to 10 minutes. The plates were then developed with a Kodak D10 developer for 3 minutes and fixed with Kodak F5 fixer for 10 minutes. Intensity measurements were done using a Jarrel-Ash Microdensitometer, and calculations of Seidel densities from plate calibration data were done using a computer programme written in Fortran and executed on a Honeywell Bull system.

IV. RESULTS AND DISCUSSION:

1. Characteristics of the glow discharge:

1.1 Current-Voltage curves: It is important in a sputtering experiment to operate the glow discharge lamp in the abnormal glow mode, to ensure high sputtering efficiencies. We, therefore, obtained the current-voltage data for various Ar pressures ranging from 1 to 15 torr. The current-voltage characteristics are shown in Fig.4. It is clear that under our operating conditions, the voltage increases linearly with current and hence the discharge is in the abnormal glow mode, specially at lower pressures.

1.2 Effect of discharge parameters on sputtering:

For a given lamp configuration and carrier gas, which in all our

experiments was Ar, the sputtering rate and excitation in the glow discharge depend on

1) the discharge voltage,

2) the current, and

3) the pressure of Ar

Of the three factors, only two can be independently selected with the third, then being automatically fixed. In our experiments we followed the sputtering rate and the excitation processes in the glow discharge by monitoring the intensity of the iron 355.69 nm line in spectra recorded by giving two minute exposures. Though the optical method does not account for redeposition of the sputtered material on the sample, (which would be taken care of in weight loss measurements), it still gives a good estimate of the extent of sputtering, specially when looking for relative sputtering efficiencies in different experiments.

The effect of the discharge voltage, current and discharge power on sputtering rates and hence on the intensity of the iron line is given in the Figs. 5, 6 and 7. As might be expected the intensity of the iron line increases with the applied voltage, current and discharge power. These results are similar to those obtained by Boumans[1] and Fang et. al[15].

We next studied the sputtering characteristics as a function of the anode-cathode distances. We sputtered a stainless steel (SS 304) sample using anode-cathode spacings of 0.15 mm, 0.30mm and 0.60 mm, for various argon pressures, discharge voltages and currents. As before, we monitored the intensity of the iron 355.69nm line to obtain relative sputtering rates in the

different experiments. Our experiments clearly showed that the sputtering efficiency was the highest for an anode-cathode spacing of 0.15mm and an Ar pressure of about 5 torr. We therefore adopted these conditions throughout most of this work.

2. Analytical application of the glow discharge lamp:

Analysis of low alloy steels: To demonstrate the analytical capability of the glow discharge lamp, we chose a set of six certified standards obtained from the Defence Metallurgical Research Laboratory (DMRL), Hyderabad, as our test samples. These contain among other elements Ni, Cr, Mn, Mo, and Cu in an iron matrix, with the concentration of the various elements ranging from 0.2 to 4% by weight. The samples were taken in the form of discs of diameter 23mm and thickness 2 mm. They were polished with C600 fine emery, washed with soap solution, rinsed with acetone and dried.

After our experiments, we noticed that one of the samples showed excessive blackening in the sputtered area. We believe that this could have been caused by an accidental leak of air into the lamp during the experiment, causing oxidation of the sample. Hence, this sample was rejected from our data set.

We sputtered the samples employing an anode-cathode distance of 0.15mm, a voltage of 1kV, a current of 150-170 mA and an argon pressure of 5 torr. Spectra were recorded in duplicate giving a 2 minute exposure. To correct for any changes in discharge conditions between experiments, intensities of the spectral lines of the different elements were ratioed with the intensity of a suitable iron line nearby. Table 1 lists the

analytical lines of the various elements that were used in this study, together with the wavelength of the corresponding iron line used as an internal standard[16,17]. Since the concentration of iron in every sample was nearly 95%, the use of it as an internal standard is justified. A plot of the logarithm of this intensity ratio versus the logarithm of concentration of the element in the sample gave excellent linear plots as shown in Figs. 8-12. The data were fit to a straight line using the least squares technique and the fit parameters, their uncertainities, and the standard deviation of the fits are given below the corresponding figures. It should be noted that in a few cases, certain intensity measurements had to be rejected either because the line was too intense or too weak.

From the slope of the working curves shown, it is obvious that the technique exhibits rather high sensitivities for the elements studied. Though, in principle, this limits the concentration range that can be analysed using a given analytical line of the element, in actual practice the range can be suitably adjusted by a judicious choice of the analytical line of appropriate intensity.

V. MODEL TO EXPLAIN THE DIFFERENT SPUTTERING EFFICIENCIES OF VARIOUS METALS:

Work done in a number of laboratories have shown that the sputtering rates of various elements differ quite significantly from each other. Boumans[1] and Bengtson et. al [7] have studied the sputtering characteristics for a variety of metals and have fitted their data to an equation

of the form

$$q = C_q \, i \, (V - V_o) \qquad \ldots.(1)$$

where q is the sputtering rate,
i is the discharge current
V is the discharge voltage
C_q and V_o are constants that depend on the metal.

They have listed the constants C_q and V_o for a number of metals from which their sputtering rates could be calculated. We were interested to see if we could relate the sputtering rates to some property or properties of the metal.

The sputtering of an atom from the surface of a metal on bombardment by an ion depends on 1) a probability factor 2) an energy factor.

Probability factor: The probability of an ion hitting an atom on the surface is given by the atom density (atoms/cc) in the metal. This is proportional to (ρ/M), where ρ is the mass density and M is the atomic weight of the atoms constituting the metal. This has to be multiplied by R^2, where R is the metallic radius, since this determines the cross section offered by the atom during the collision. The term ($R^2\rho$/M) therefore gives the probability of an ion colliding with an atom in the metal. A similar dependence has also been discussed by Broekaert [6].

Energy factor: On collision by an ion, the atom has to free itself from the binding forces in the solid, for it to be sputtered. These binding forces vary from metal to metal and is chiefly responsible for the different sputtering rates of the various metals. We believe that a good estimate of the binding forces in the solid is given by the heats of sublimation of the solid. Though the process of sublimation is not a stimulated

process as sputtering is, the forces that the atom has to work against is similar in both cases. Sublimation may in fact be considered as an 'auto-sputtering' phenomenon. The sputtering rate of a metal, S, (wt/sec) shall, therefore, be inversely proportional to $(\Delta H_s/M)$, where ΔH_s is the heat of sublimation for the metal in kcal/mole, and M is the atomic weight. The term $\Delta H_s/M$ is essentially the heat of sublimation per gram of the metal. Combining the probability and the energy terms, the sputtering rate, S, is given by

$$S \propto R^2 \rho / \Delta H_s \quad .... (2)$$

Table 2 gives the sputtering rate, S, for ten different elements calculated using the constants C_q and V_o given by Boumans[1] and Bengtson et. al[7], and assuming a discharge voltage of 1kV and a current of 100 mA. Also listed are the ΔH_s values for the different metals[18], their metallic radii and densities[19]. A plot of S versus the term $(R^2 \rho / \Delta H_s)$ is shown in Fig. 13. The correlation is remarkably good, with a correlation coefficient of 0.95.

It is interesting to note that Al has a poorer sputtering rate than Cu, even though both metals have about the same heat of sublimation. It is the low density of Al, and hence the lower probability of sputtering, that makes Al a poor sputterer. W, on the other hand sputters about as good as Cu, eventhough it has a much higher heat of sublimation, due mainly to its high density and hence a favourable probability factor. Zn sputters excellently because of its low heat of sublimation. Sn also turns out to be a good sputterer, gaining mainly by its

larger metallic radius.

Our model is based entirely on the data given in Ref. 1 and 7. Work is in progress in our laboratory to generate data on sputtering rates for a number of metals (including the ones listed in Table 2), to confirm the validity of our model.

Acknowledgement: The authors are grateful tc Dr.C.K.Mathews, Head, Radiochemistry Programme, for his keen interest and constant encouragement during the course of this work.The authors gratefully acknowledge the enthusiastic assistance of Mr. A. Veerapandian, in the fabrication of the glow discharge lamp.

REFERENCES

1. P.W.J.M. Boumans, Analytical Chemistry, 44, 1219 (1972).

2. M.E. Waitlevertch and J.K. Hurwitz, Applied Spectrosc., 30, 510 (1976).

3. J.M. Brackett and T.J. Vickers, Spectrochim. Acta, 37B, 841 (1982).

4. N.P. Ferreira, J.A. Strauss and H.G.C. Human, Spectrochim. Acta, 38B, 899 (1983).

5. B.M. Patel and J.D. Winefordner, Applied Spectrosc., 40, 667 (1986).

6. J.A.C. Broekaert, J. Analytical Atomic Spectrometry, 2, 537 (1987).

7. A. Bengtson and L. Danielsson, Thin Solid Films, 124, 231 (1985).

8. M.G. Barker and I.E. Schreinlehner, Surface and Interface Analysis, 9, 371 (1986).

9. J. Pons-Corbeau,J.P. Cazet, J.P. Moreau, R. Berneron and J.C. Charbonnier, Surface and Interface Analysis, 9, 21 (1986).

10. F. Llewellyn-Jones, "The glow discharge and an introduction to plasma physcis", John Wiley & Sons Inc., New York, (1966).

11. W. Grimm, Spectrochim. Acta, 23B, 433 (1967).

12. R.A. Kruger, R.M. Bombelka and K. Laqua, Spectrochim. Acta, 35B, 581 (1980).

13. S. Caroli, J. Analytical Atomic Spectrometry, 2, 661 (1987).

14. R. Mavrodineanu, J. Research of the NBS, 89, 143 (1984).

15. D. Fang and R.K. Marcus, Spectrochim. Acta, 43B, 1451 (1988).

16. CRC Handbook of Chemistry and Physics, 59th Edition, CRC Press, (1978-1979).

17. MIT Wavelength Tables, comp. G.R. Harrison, MIT Press, (1982).

18. R.E. Honig, The Characterization of High-Temperature Vapors (Appendix A), Ed. J.L. Margrave, 482-486, John Wiley & Sons, Inc., New York.

19. G.H. Aylward and T.J.V. Findlay, SI Chemical Data, pp. 6-13, John Wiley & Sons, (1977).

Table 1

EMISSION WAVELENGTHS USED FOR THE DIFFERENT ELEMENTS ALONG WITH THE WAVELENGTHS OF IRON USED AS AN INTERNAL STANDARD.

Element	Analytical Wavelength (nm)	Wavelength of Int. Std. (nm)
Ni	305.0	304.0
Mn	403.3	400.5
Cr	425.4	430.8
Mo	386.4	386.5
Cu	324.7	344.0

Table 2

SPUTTERING RATES[1,7], HEATS OF SUBLIMATION[17], METALLIC RADII AND DENSITIES[18] FOR THE VARIOUS METALS.

Metal	Sputtering Rate (μg/sec)	Metallic Radius (A)	Density (g/cc)	Heat of Sublimation (kcal/gmol)	$\frac{R^2\rho}{\Delta H_s}$ (x100)
Al	6.5	1.43	2.70	78.0	7.08
Cr	13.1	1.30	7.19	94.9	11.84
Fe	16.8	1.26	7.86	99.55	12.14
Mo	27.3	1.39	10.2	158.7	11.89
Ni	30.8	1.24	8.9	102.67	13.54
W	53.7	1.41	19.3	201.8	17.95
Ta	55.1	1.49	16.6	186.9	18.16
Cu	57.5	1.28	8.96	80.53	18.23
Sn	93.0	1.62	7.30	72.1	23.09
Zn	119.3	1.38	7.14	31.25	40.42

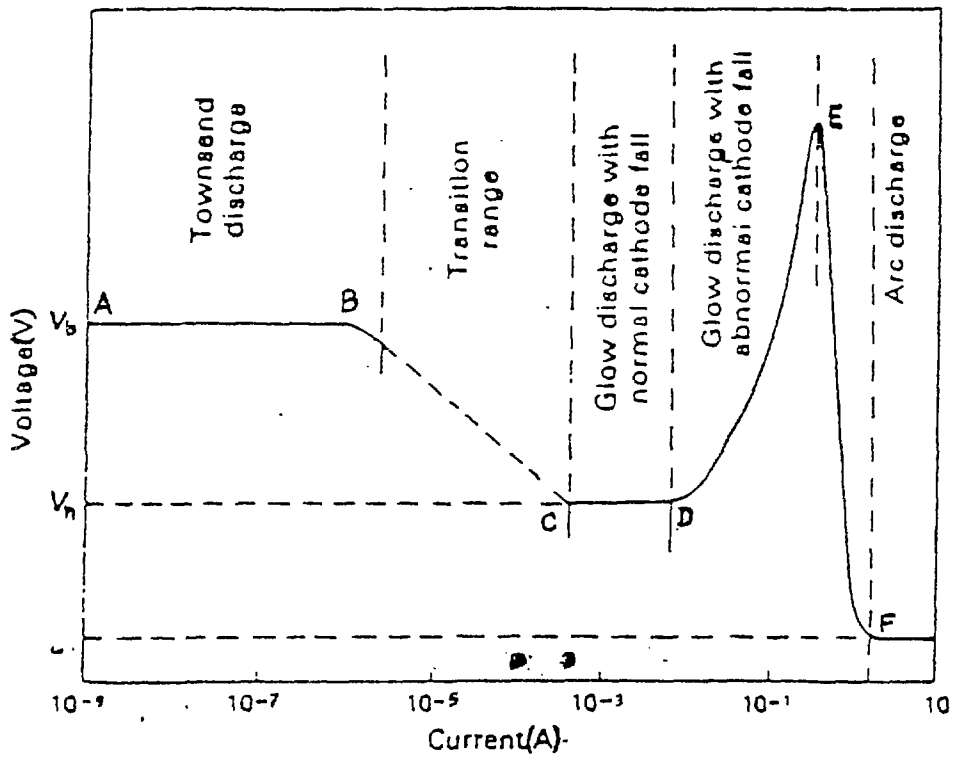

Fig 1. Characteristic of a self-sustaining gas discharge (Reproduced from Ref.6)

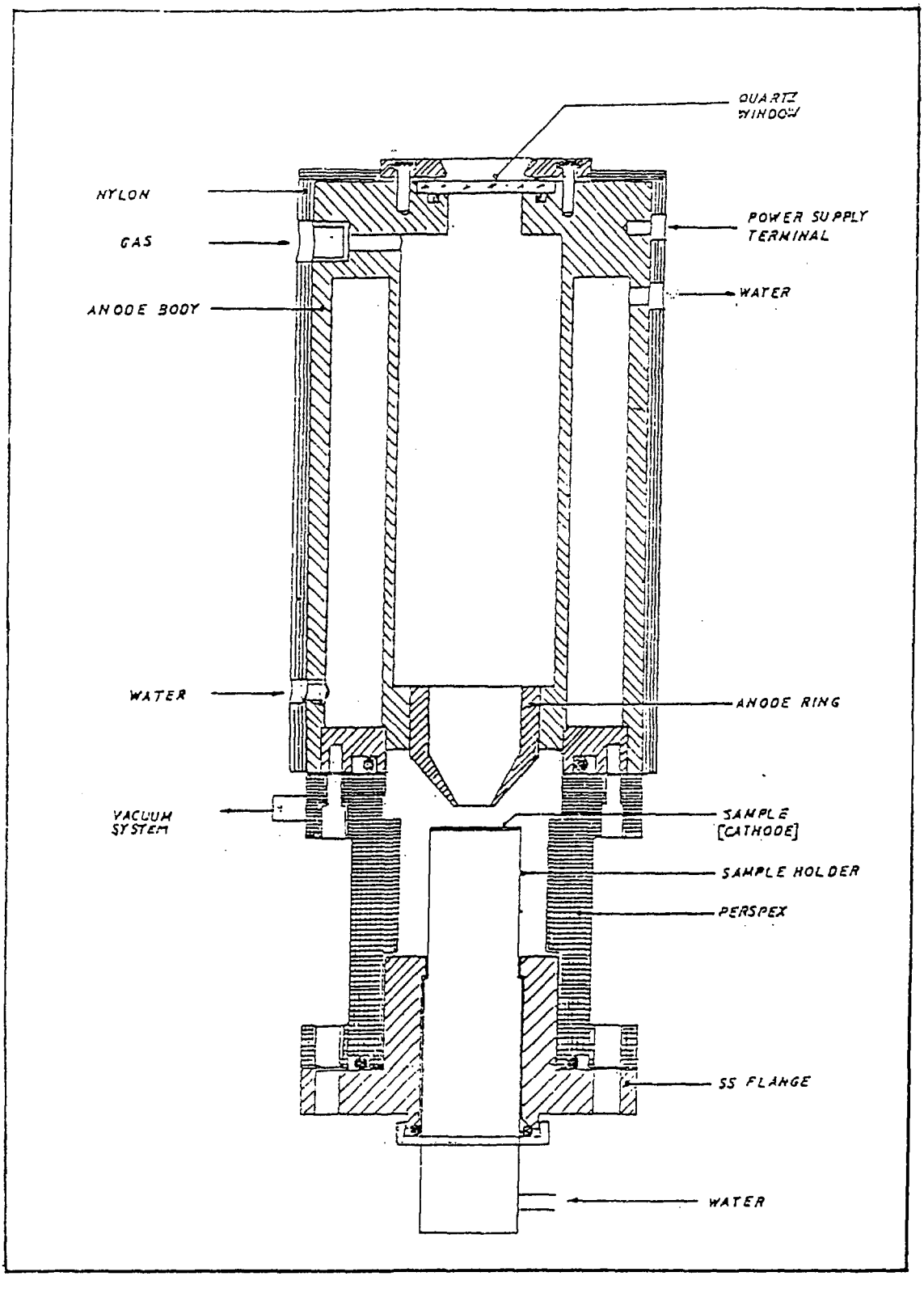

Fig 2. Schematic diagram of the Glow-discharge lamp.

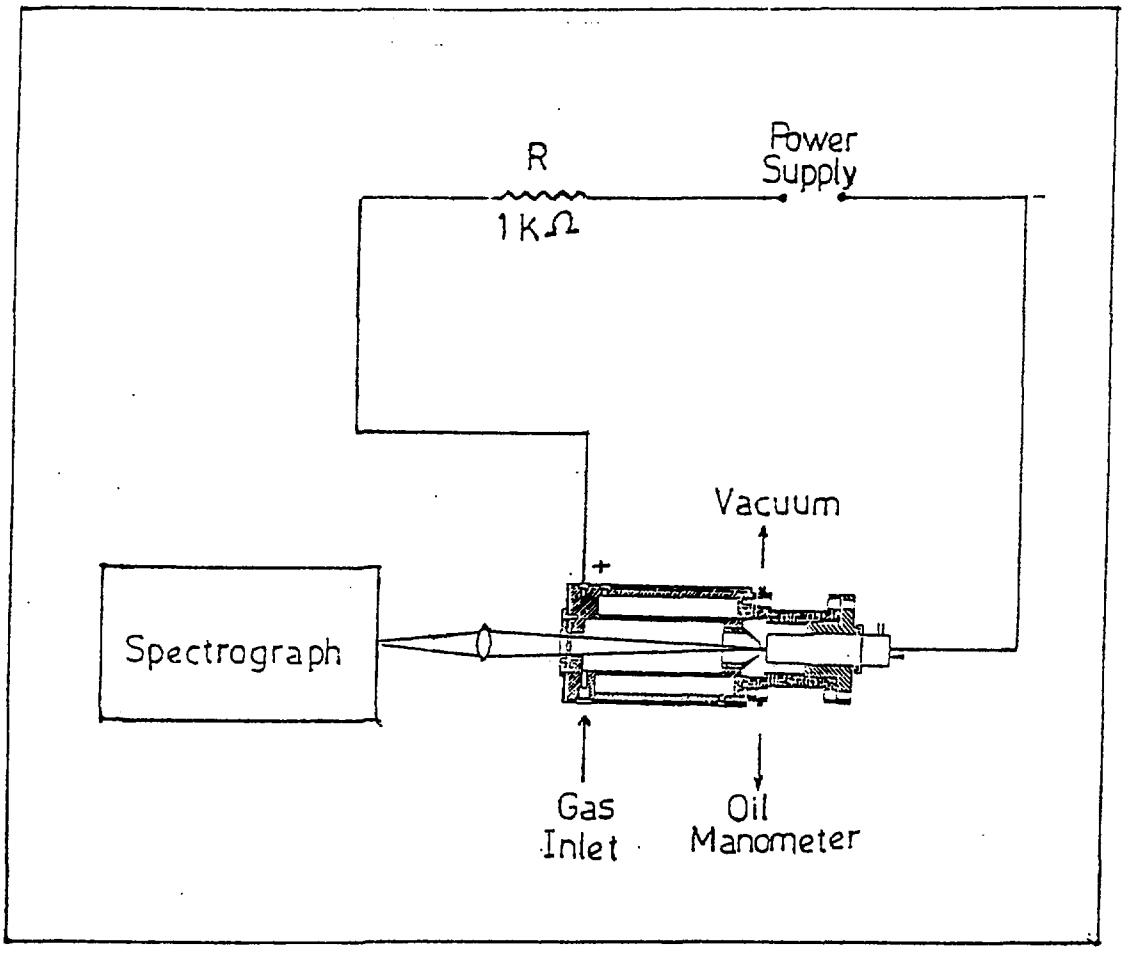

Fig 3. Schematic of the Glow-discharge setup.

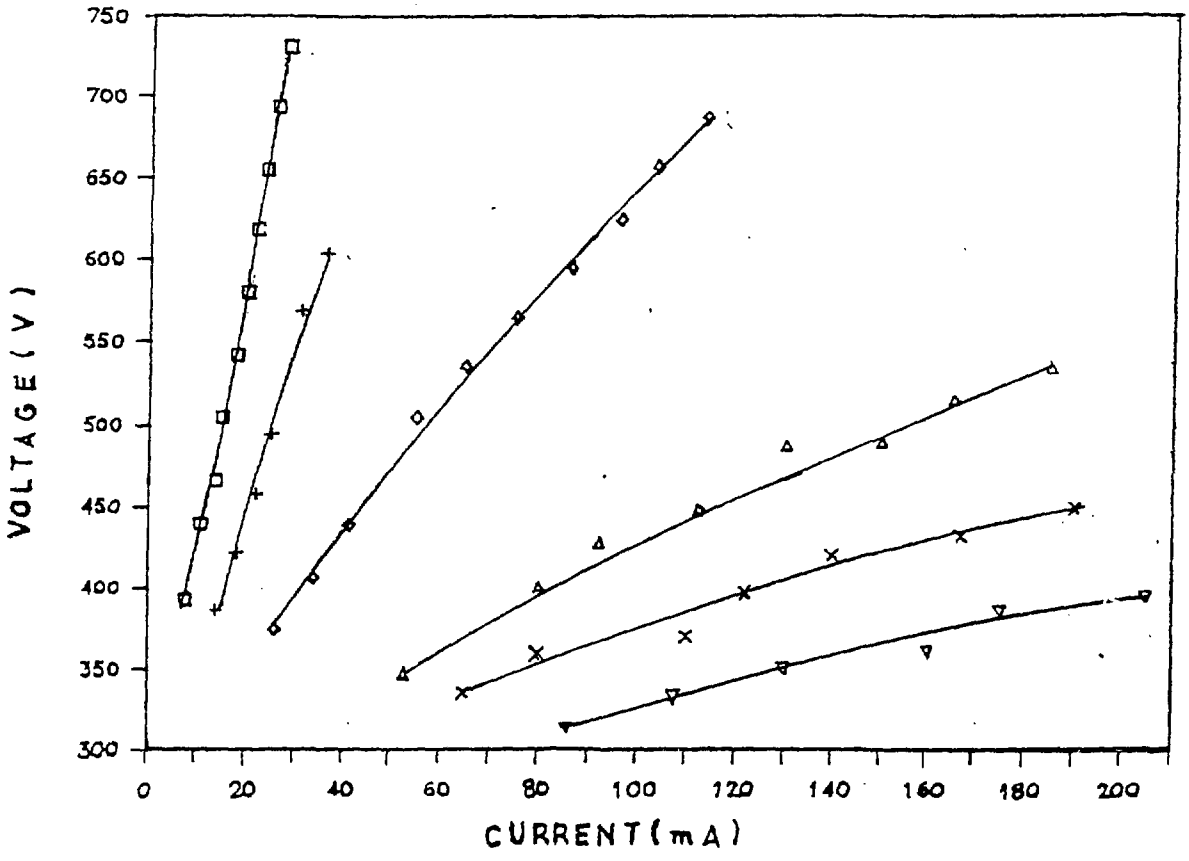

Fig 4. Current-voltage characteristics of the discharge for various pressures of Argon. (□ : 1 torr, + : 3 torr, ◇ : 5 Torr, △ : 8 Torr, × : 11 torr, ▽ : 15 torr)

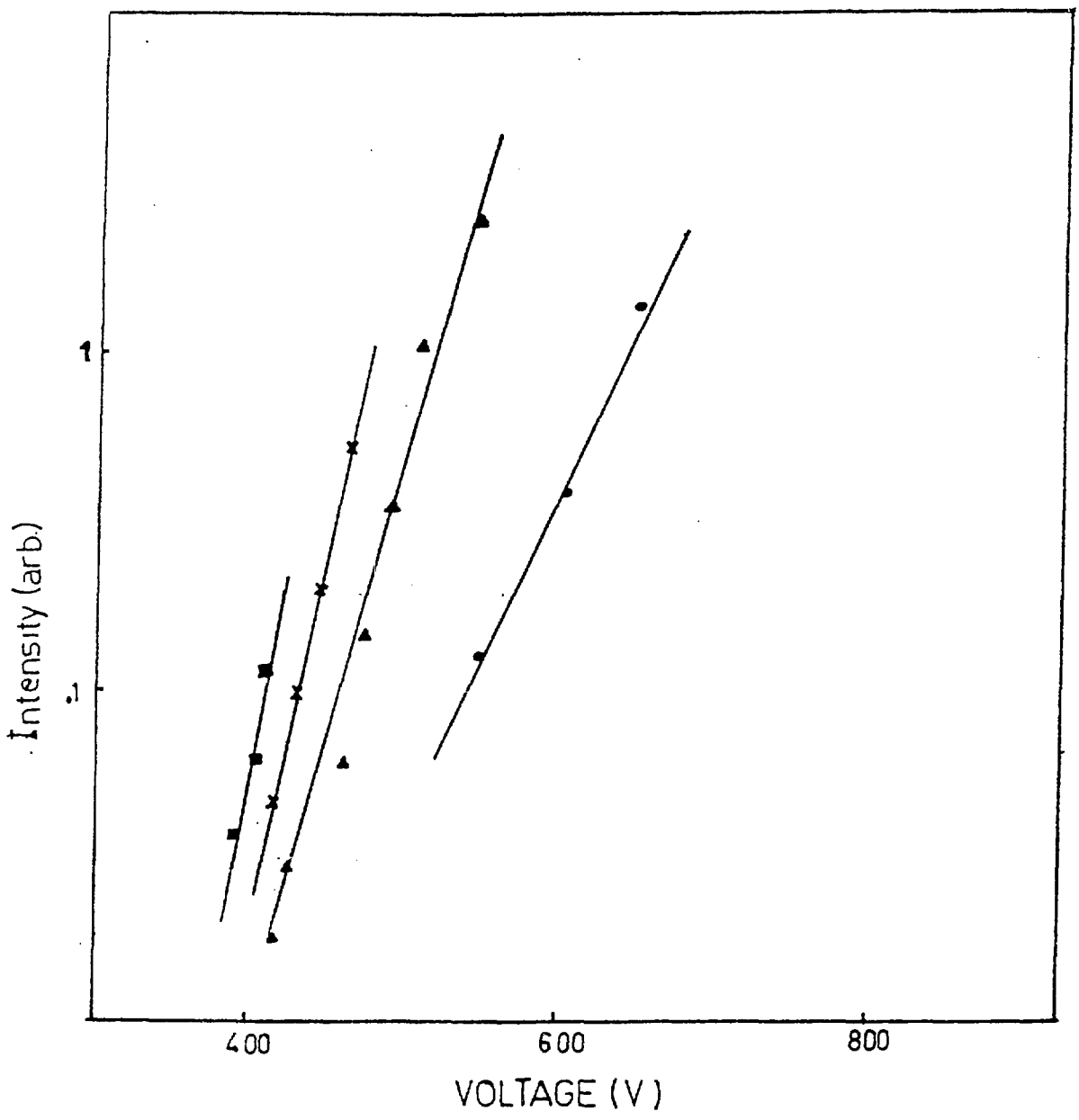

Fig 5. Plot of the logarithm of the intensity of the iron line at 355.69 nm as a function of the discharge voltage for various pressures of argon. (● : 4 torr, ▲ : 7 torr, × : 10 torr, ■ : 13 torr)

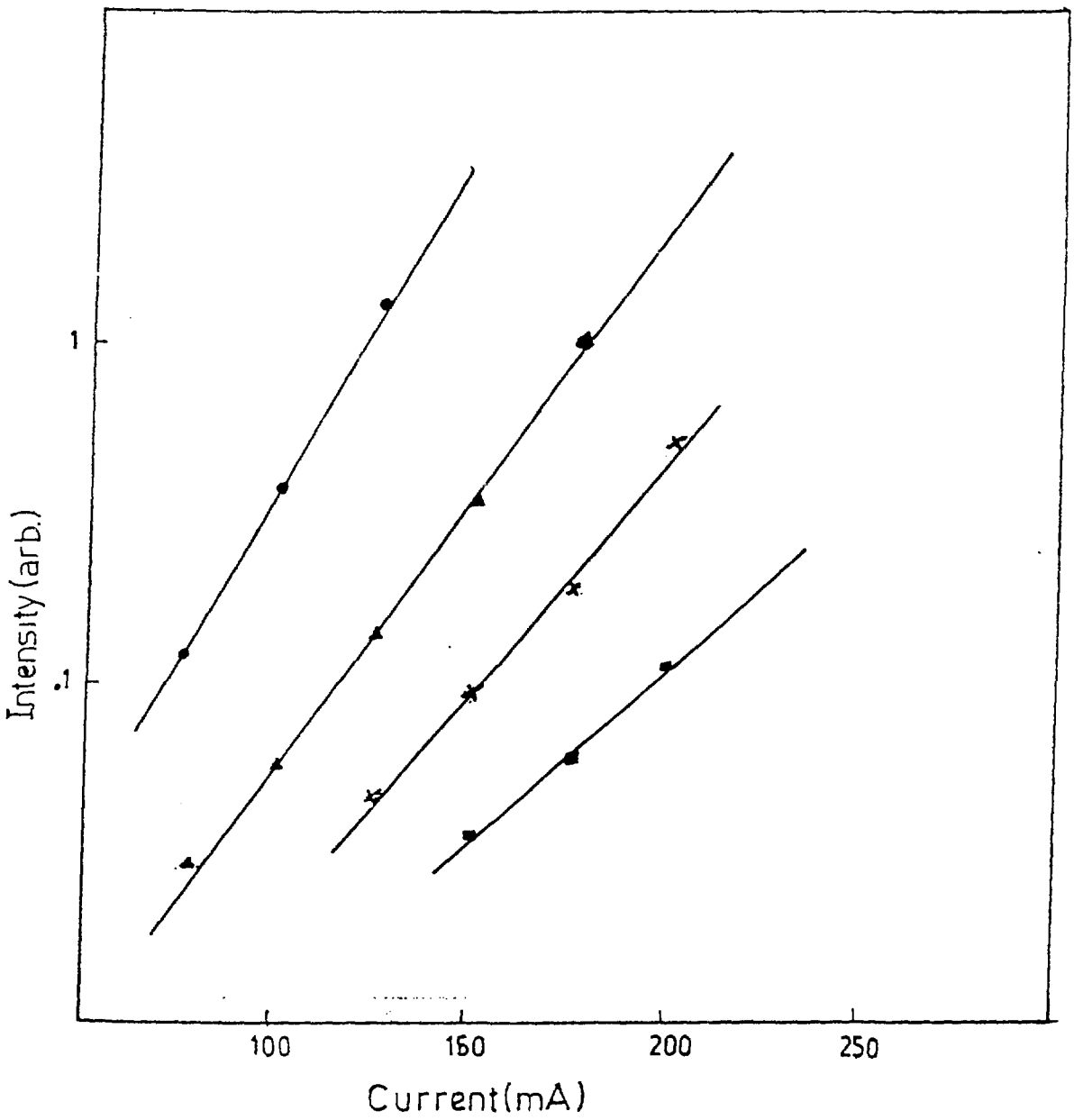

Fig 6. Plot of the logarithm of the intensity of the iron line at 355.69 nm as a function of current for various pressures of argon. (● : 4 torr, ▲ : 7 torr, × : 10 torr, ■ : 13 torr)

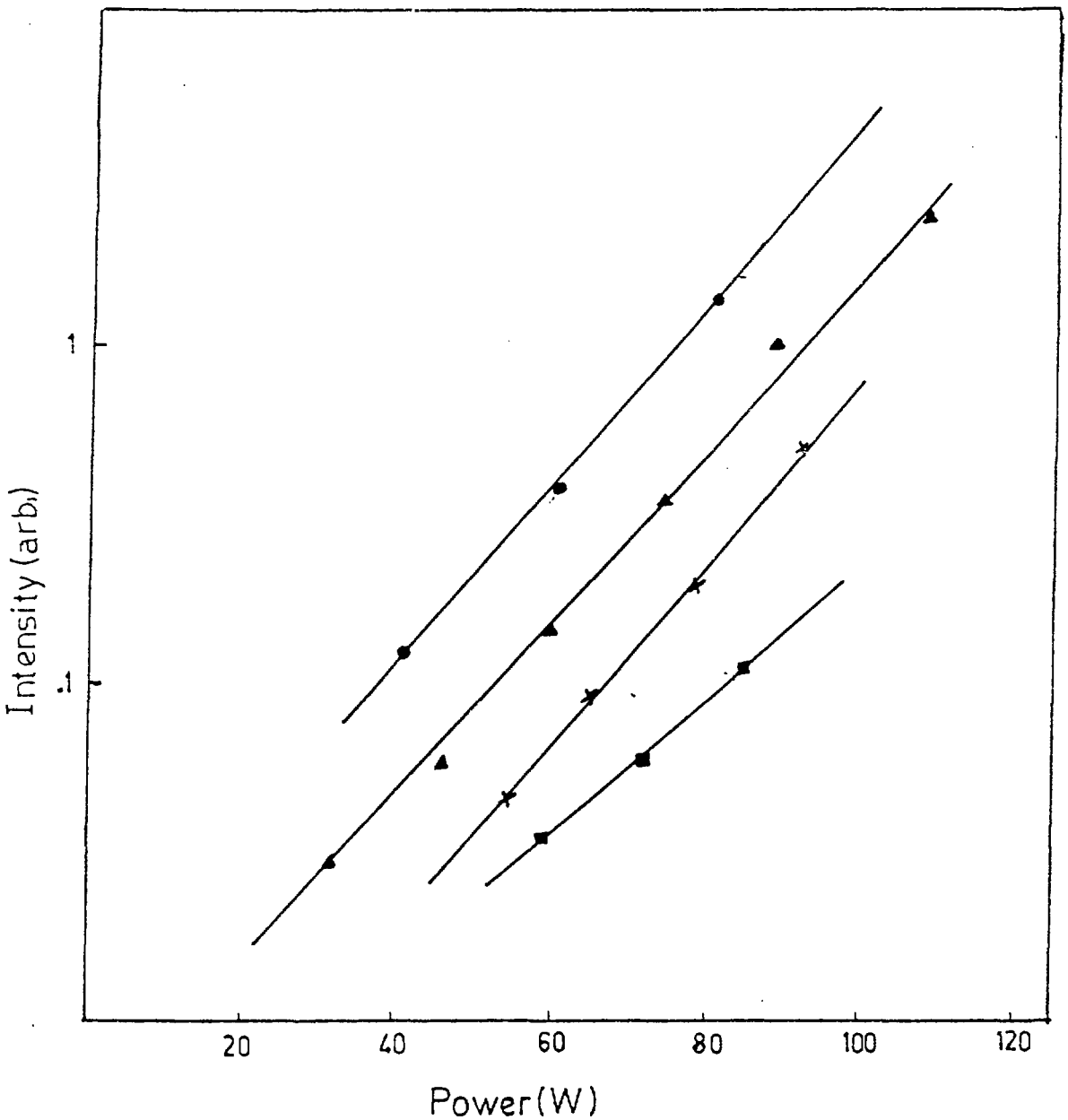

Fig 7. Plot of the logarithm of the intensity of the iron line at 355.69 nm as a function of discharge power for various pressures of argon. (● : 4 torr, ▲ : 7 torr, × : 10 torr, ■ : 13 torr)

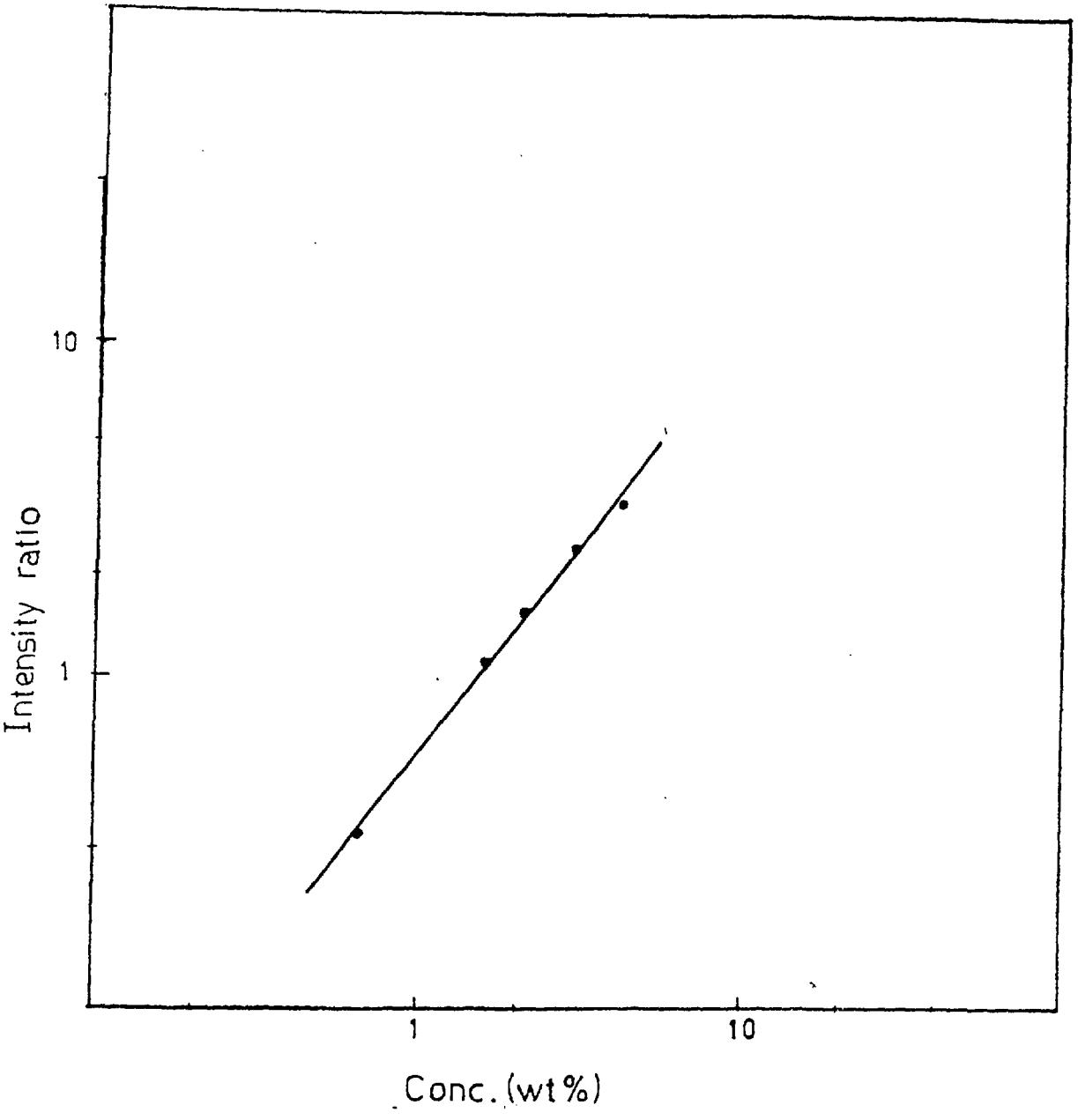

Fig 8. Plot of the logarithm of intensity ratio (Ni 305.0nm/Fe 304.0nm) versus logarithm of nickel concentration in the solid. Data fit to Y = a+bx. Fit parameters with standard errors in brackets are: a = -0.22823 (0.01098); b = 1.2778 (0.02817) standard deviation of the fit = 2.406 E-02

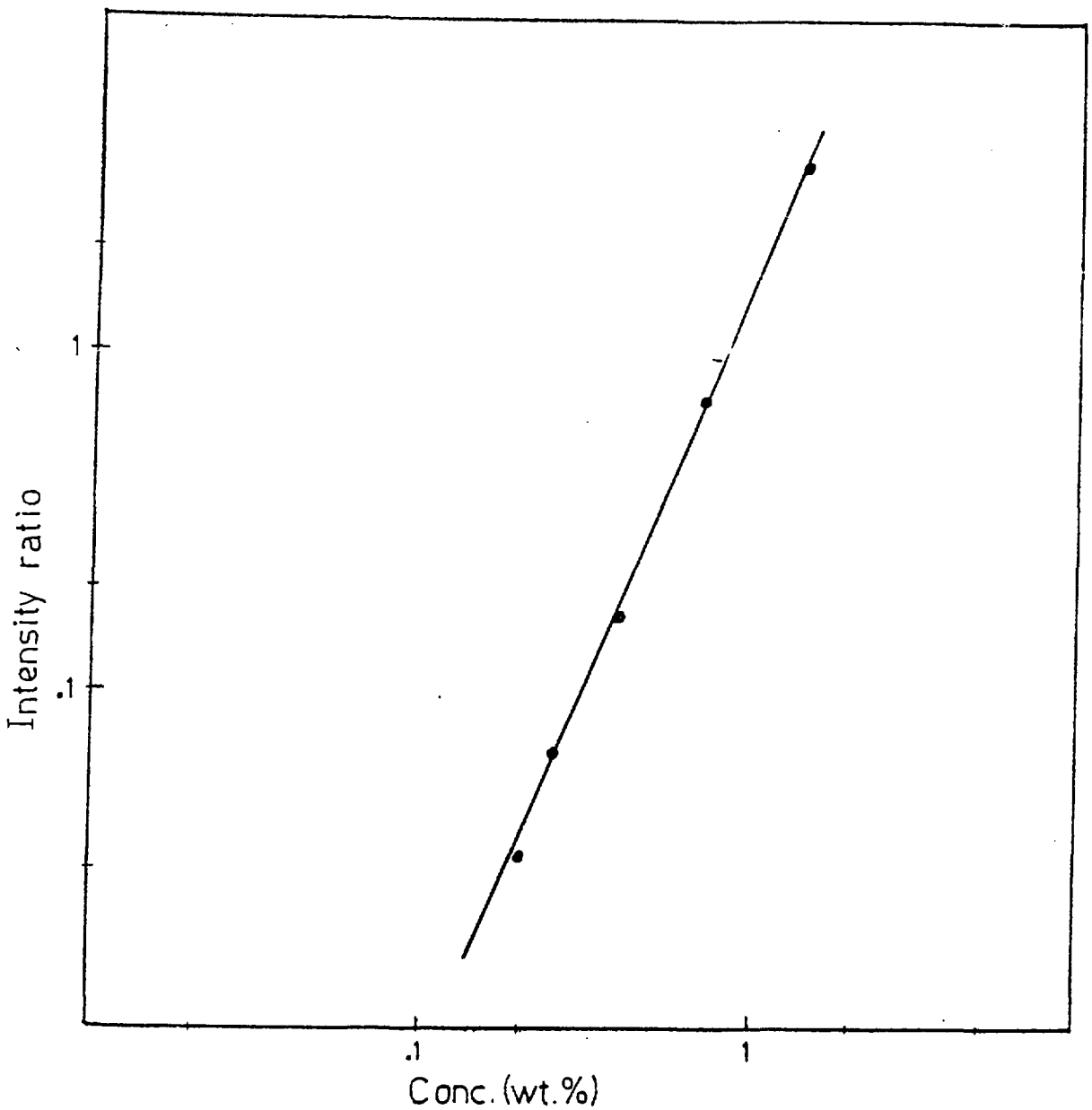

Fig 9. Plot of the logarithm of intensity ratio (Mn 403.3nm/Fe 400.5nm) versus logarithm of manganese concentration in the solid. Data fit to Y = a+bx. Fit parameters with standard errors in brackets are: a = 0.21628 (0.01678); b = 2.3914 (0.03645) standard deviation of the fit = 3.5629 E -02

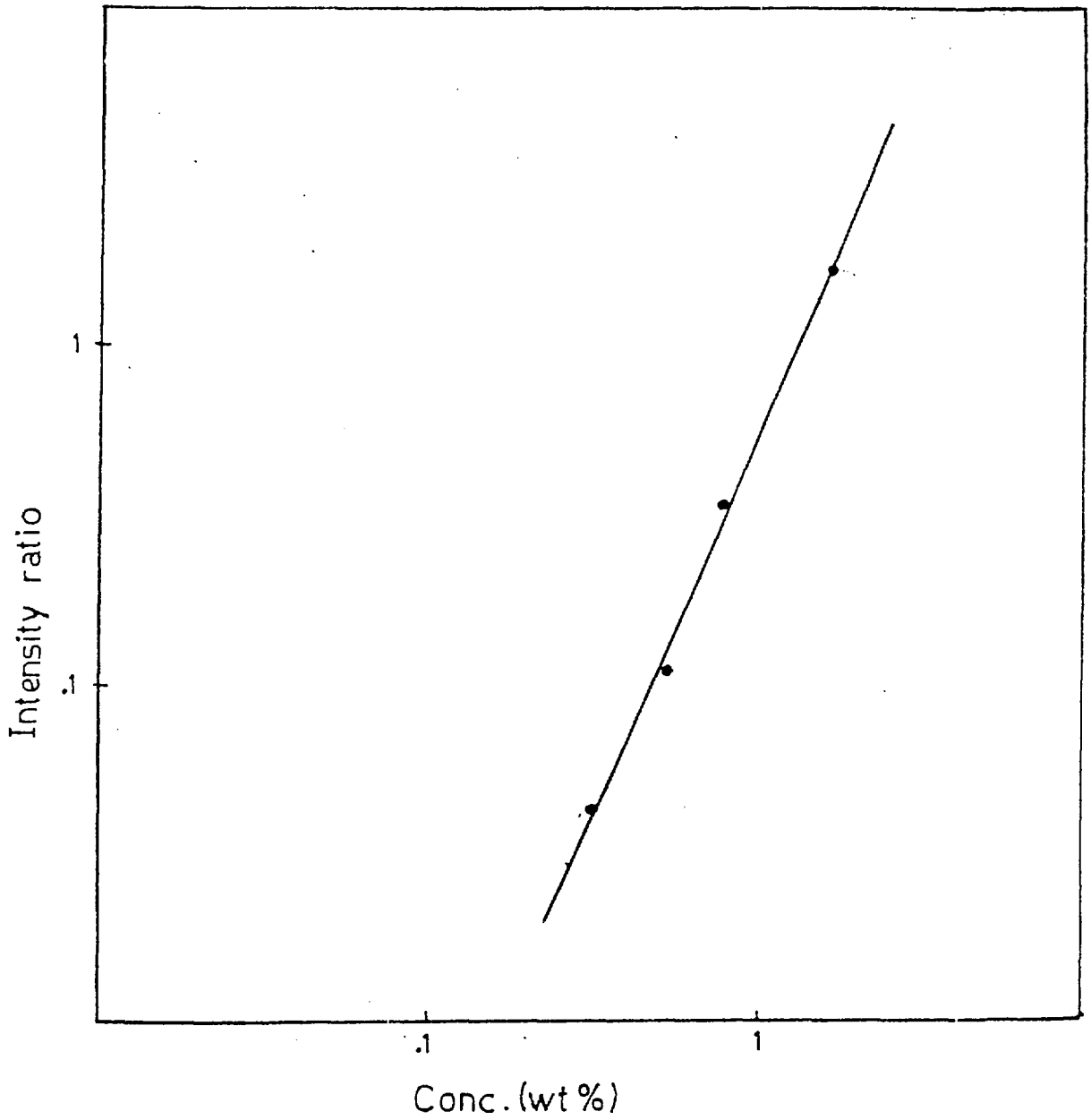

Fig 10. Plot of the logarithm of intensity ratio (Cr 425.4nm/Fe 430.8nm) versus logarithm of chromium concentration in the solid. Data fit to Y = a+bx. Fit parameters with standard errors in brackets are: a = -0.19914 (0.02289); b = 2.3046 (0.07231) standard deviation of the fit = 5.1393 E-02

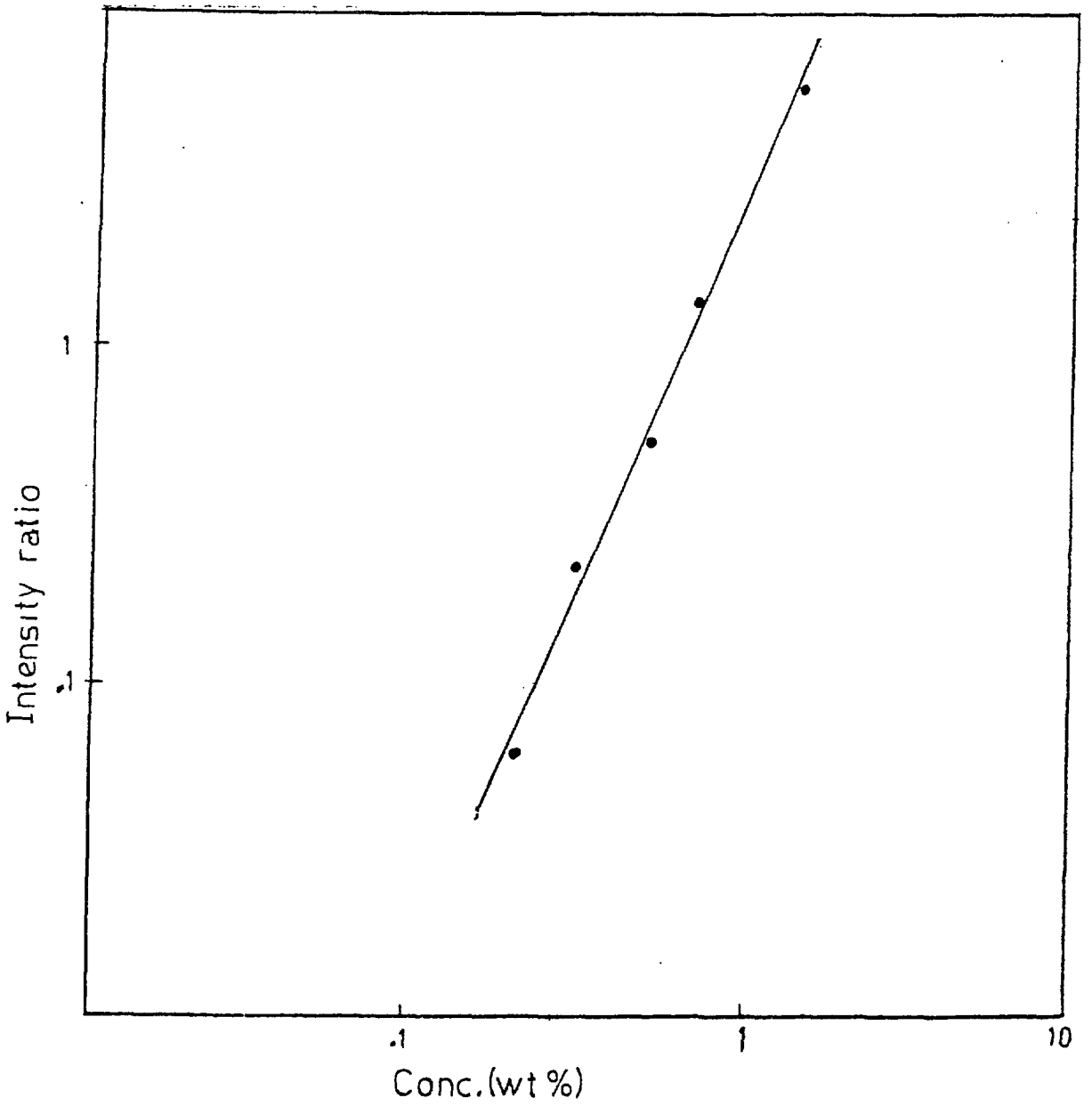

Fig 11. Plot of the logarithm of intensity ratio (Mo 386.4nm/Fe 386.5nm) versus logarithm of molybdenum concentration in the solid. Data fit to Y = a+bx. Fit parameters with standard errors in brackets are: a = 0.39849 (0.02968); b = 2.2244 (0.07034) standard deviation of the fit = 6.7233 E-02

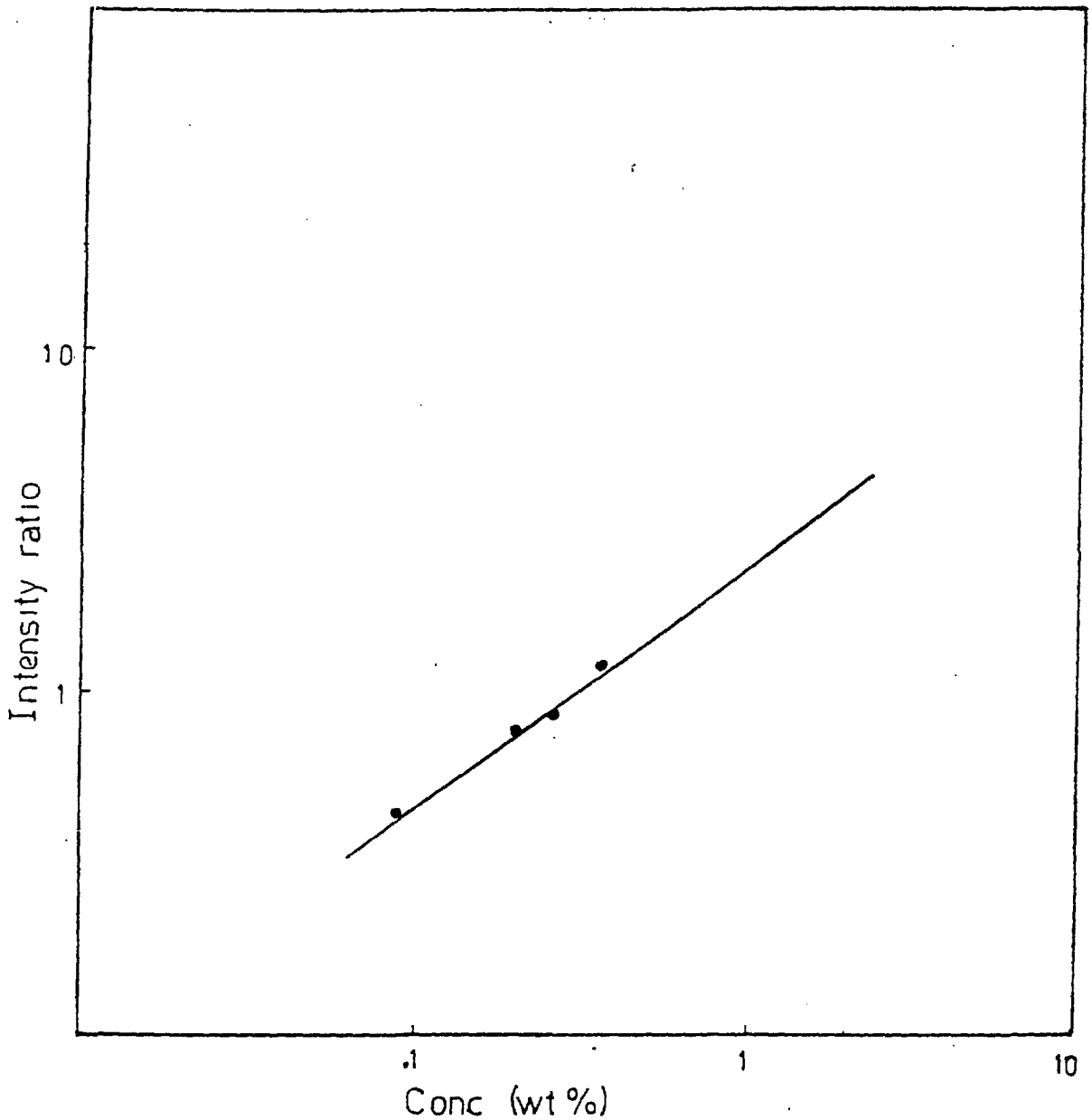

Fig 12. Plot of the logarithm of intensity ratio (Cu 324.7nm/Fe 344.0nm) versus logarithm of copper concentration in the solid. Data fit to Y = a+bx. Fit parameters with standard errors in brackets are: a = 0.52568 (0.064978); b = 0.88766 (0.09251) standard deviation of the fit = 7.0586 E-02

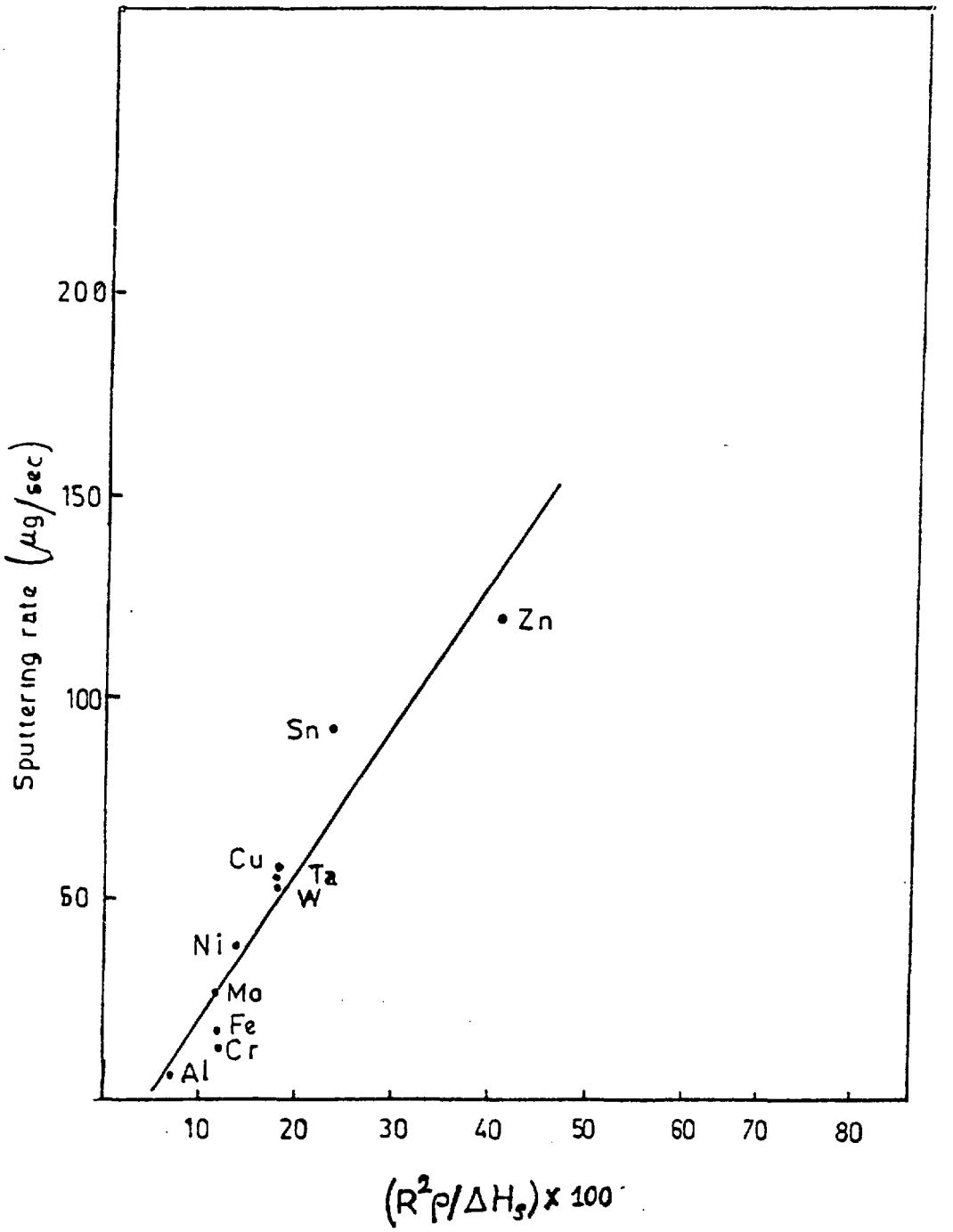

Fig 13. Plot of the sputtering rate of various metals versus $(R^2 \rho / \Delta H_s)$.